THE JOURNAL OF PHYSICAL CHEMISTRY B

Article

pubs.acs.org/JPCB

Polar Switching in Trialkylbenzene-1,3,5-tricarboxamides

Carel F. C. Fitié,[†] W. S. Christian Roelofs,[‡] Pieter C. M. M. Magusin,[§] Michael Wübbenhorst,[∥] Martijn Kemerink,[‡] and Rint P. Sijbesma*,[†]

[†]Laboratory of Macromolecular and Organic Chemistry, Eindhoven University of Technology, P.O. Box 513, 5600 MB Eindhoven, The Netherlands

[‡]Department of Applied Physics, Eindhoven University of Technology, P.O. Box 513, 5600 MB, Eindhoven, The Netherlands

[§]Schuit Institute of Catalysis, Eindhoven University of Technology, P.O. Box 513, 5600 MB Eindhoven, The Netherlands

[∥]Laboratory of Acoustics and Thermal Physics, Department of Physics and Astronomy, Katholieke Universiteit Leuven, Celestijnenlaan 200D, B-3001 Leuven, Belgium

Supporting Information

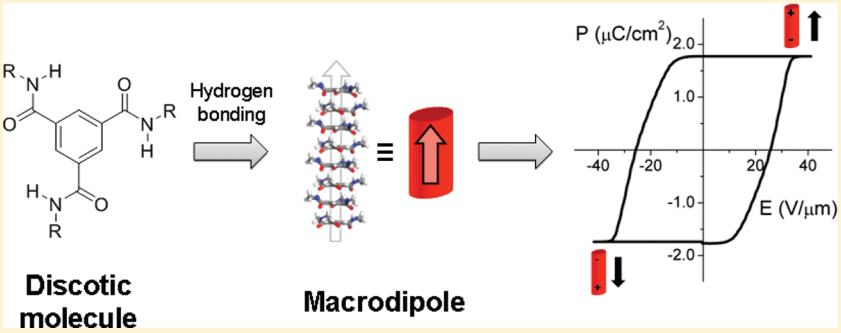

ABSTRACT: The hydrogen-bonded hexagonal columnar LC (Col_{hd}) phases formed by benzene-1,3,5-tricarboxamide (BTA) derivatives can be aligned uniformly by an electric field and display switching behavior with a high remnant polarization. The polar switching in three symmetrically substituted BTAs with alkyl chains varying in length between 6 and 18 carbon atoms (**C6**, **C10**, and **C18**) was investigated by electro-optical switching experiments, dielectric relaxation spectroscopy (DRS), and solid-state NMR. The goal was to characterize ferroelectric properties of BTA-based columnar LCs, which display a macroscopic axial dipole moment due to the head-to-tail stacking of hydrogen-bonded amides. The Col_{hd} phase of all three BTAs can be aligned uniformly by a dc field ~30 V/μm. Moreover, **C10** and **C18** display extrinsic polar switching characterized by a remnant polarization and coercive field of 1−2 μC/cm^2 and 20−30 V/μm, respectively. In the absence of an external field, the polarization is lost in 1−1000 s, depending on device details and temperature. DRS revealed a columnar glass transition in the low-temperature region of the LC phase related to collective vibrations in the hydrogen-bonded columns that freeze out below 41−54 °C. At higher temperatures, a relaxation process is present originating from the collective reorientation of amide groups along the column axis (inversion of the macrodipole). Matching activation energies suggest that the molecular mechanism underlying the polar switching and the R-processes is identical. These results illustrate that LC phases based on BTAs offer the unique possibility to integrate polarization with other functionalities in a single nanostructured material.

1. INTRODUCTION

Organic thin films with a large remnant polarization hold great promise for application in diodes and nonvolatile memory devices.[1,2] One class of organic materials that is of specific interest for such applications are ferroelectric columnar liquid crystals (LCs) featuring stable, switchable polarization along the column axis. These LC phases have received considerable attention because of their potential application in ultra-high-density memory devices in which a single column can ultimately function as a memory element through manipulation of its macroscopic polarization.[3] Additionally, the potential ferroelectric behavior of achiral columnar LCs with axial polarity is of fundamental interest, because the most abundant and best known examples of organic materials with ferroelectric properties are found in polar LC phases formed by chiral molecules.[4−7] However, despite several research efforts directed toward this goal, ferroelectric behavior in achiral columnar LCs has not been observed.[3,8−13]

Previously, we have used discotic molecules with a benzene-1,3,5-tricarboxamide (BTA) core to design nanostructured columnar LC phases incorporating several polymeric species and we have reported initial results for polar switching in a simple trialkyl BTA.[14−16] The latter study showed that the polar order induced in the hydrogen-bonded LC phase can be

Received: September 13, 2011
Revised: March 4, 2012
Published: March 7, 2012

 © 2012 American Chemical Society

frozen by crystallization of the alkyl chains in the periphery of the columns, yielding thin films with remnant polarization and an unprecedented high surface potential as shown by scanning Kelvin probe microscopy (SKPM). The results of these previous studies show that BTA-based columnar LC phases offer a potential route to integrate permanent polarization with other functionalities in a single nanostructured material and prompted us to investigate the dielectric and ferroelectric properties of BTAs in more detail in the current contribution.

BTAs are easy to synthesize and they are known to form columnar hexagonal LC phases over a wide temperature range (50−215 °C) when side chains of sufficient length are attached.[17,18] Apart from the LC phase, BTAs have been studied extensively in the solid state,[19−21] as organogelators[22−25] and as a model system to study self-assembly mechanisms.[26−30] These studies have consistently shown that BTAs form supramolecular columnar assemblies through 3-fold hydrogen bonding between the amide groups connected to the core. From crystal structures, molecular modeling, and X-ray scattering studies on the columnar LC phase, it is known that the three amide bonds of each BTA point in the same direction and are rotated approximately 40° out of plane with respect to the central benzene ring in the supramolecular columns. This arrangement results in an overall helical columnar structure in which two neighboring BTAs are rotated about 60° relative to each other with a core separation of around 0.35 nm.[19,20,29,31] The effective electric dipole moment of the three amide groups in each individual BTA is directed perpendicular to the benzene ring for both the left- and right-handed helical structure. Due to head-to-tail stacking of the BTAs in the supramolecular columns, these individual dipole moments add up and result in a large macroscopic dipole pointing along the column axis (Scheme 1).

Scheme 1. Chemical Structures of the BTAs Investigated in This Work (left) and an Illustration of the Macrodipole along the Column Axis (right) Resulting from the Hydrogen-Bonded Stacking between BTA Cores[a]

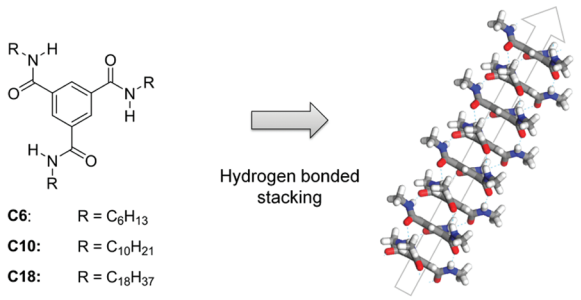

[a]BTAs with three methyl substituents are shown in stick rendering.

The presence of this macrodipole has been verified experimentally in gels formed by BTAs in *n*-decane through a combination of rheology and dielectric relaxation spectroscopy (DRS).[22,23] In addition, Sugita and co-workers recently reported on the ferroelectric properties of BTA derivatives from room temperature up to 100 °C in three separate contributions.[32−34] Even though the results obtained in these studies for different BTAs were not consistent and the exact structure of the phases was not completely clear, some of the measurements indicated a significant ferroelectric effect.

Here we report on the dielectric relaxations and the characterization of polar switching in a series of three symmetric trialkyl BTAs with alkyl chains varying in length between 6 and 18 carbon atoms (**C6**, **C10**, **C18**, Scheme 1). In many ways, the switching behavior resembles ferroelectric switching; however, because of the limited retention of the polarized state that will be discussed below, we choose to refer to the switching process as "polar switching".

This paper is structured as follows: first, the synthesis, phase behavior, and the structure of the LC phases formed by the three BTAs under investigation are treated briefly. Second, with the LC structure established, polar switching for **C10** and **C18** in the LC phase will be demonstrated on the basis of several electro-optical experiments. Finally, the results of a DRS study aimed at further characterizing the molecular origin of the polar switching in BTAs are presented.

2. RESULTS AND DISCUSSION

2.1. Synthesis, Phase Behavior, and LC Structure. The three BTAs with different side-chain lengths were synthesized in a one-step procedure starting from benzene-1,3,5-tricarboxylic acid chloride and the corresponding primary amines. The identity and purity of the products were confirmed by ^{1}H and ^{13}C NMR spectrometry, MALDI-TOF mass spectrometry, and elemental analysis. The phase behavior of all three compounds was investigated by differential scanning calorimetry (DSC) experiments. The phase transition temperatures and the transition enthalpies were determined from the first cooling and second heating traces in DSC and are tabulated in Table 1. The structure of the LC phases formed by these BTAs was assigned based on wide-angle X-ray scattering (WAXS) measurements.[35]

The transition from the hexagonal columnar LC phase to the isotropic liquid takes place around 210 °C for all three compounds in the heating run and occurs at approximately the same temperature upon cooling. These transition temperatures and corresponding enthalpies (15−22 kJ/mol) are comparable to the literature values reported by Matsunaga et al.[17,18] Upon heating, the transition from the crystalline to the LC phase occurs well above room temperature for **C6** and **C18** (67 and 79 °C, respectively) and slightly below room temperature for **C10** (19 °C). The transition temperatures from the crystalline to the LC phase were based on the second DSC cycle and are considerably lower for **C6** and **C10** than the corresponding literature values, which are based on first heating runs. During the cooling runs in the DSC experiments, all three BTAs crystallize with a clearly detectable supercooling effect of 5−20 °C. Interestingly, we found that **C6** exhibits a third, very weak transition around 165 °C corresponding to the transition from a rectangular to hexagonal columnar LC phase that was not reported by Matsunaga and co-workers.

2.2. Polar Switching Experiments. The investigation of the electric field alignment and the possible ferroelectric properties of the columnar LC phase formed by the BTAs requires a sample environment that allows simultaneous optical and electrical access to the samples. For this purpose, commercial glass LC cells were selected with a constant cell spacing of 5 μm that were coated with two transparent electrodes (indium tin oxide). All samples for the experiment described in this section were prepared by introducing the BTAs in the LC cells in the isotropic state under reduced pressure (230 °C, 20 mbar).

2.2.1. BTAs Align Uniformly under Dc Fields. The columnar LC phases formed by BTAs were aligned with an electric field

dx.doi.org/10.1021/jp300008f | J. Phys. Chem. B 2012, 116, 3928−3937

Table 1. Phase Behavior of the BTAs with Different Alkyl Side Chains C6, C10, and C18

compd		T, °C (ΔH, kJ/mol)[a]						
C6	heating	Cr	67 (1.7)	Col_{rd}	167 (0.4)	Col_{hd}	210 (21.7)	I
	cooling	Cr	40 (3.3)	Col_{rd}	164 (0.5)	Col_{hd}	209 (19.9)	I
C10	heating	Cr	19 (18.0)			Col_{hd}	211 (17.9)	I
	cooling	Cr	14 (15.9)			Col_{hd}	211 (17.2)	I
C18	heating	Cr	79 (74.1)[b]			Col_{hd}	210 (16.0)	I
	cooling	Cr	60 (90.8)			Col_{hd}	209 (14.6)	I

[a]Onset temperatures and transition enthalpies are reported based on the first cooling and second heating run in DSC (10 °C/min). The observed phases are identified by following abbreviations: Cr = crystalline, Col_{rd} = disordered rectangular columnar LC, Col_{hd} = disordered hexagonal columnar LC, I = isotropic liquid. [b]The main melting transition is preceded by a very broad and weak transition with a peak at 63 °C.

by heating the samples to 150 °C and applying a dc field of 30 V/μm. For **C10**, visual inspection of the sample by polarizing optical microscopy (POM) revealed that the columns were aligned perpendicular to the electrodes after approximately 5 min as evidenced by a black texture in the electrode area of the LC cell (Figure 1). The alignment for **C18** samples proceeded

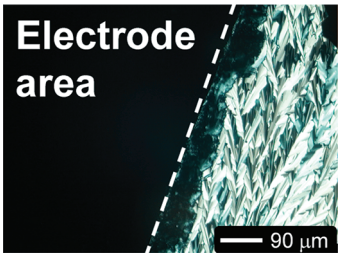

Figure 1. POM micrograph of aligned **C10** (150 °C). The white dashed line indicates the electrode edge.

easily under these conditions as well and was generally complete within 5 min. In the rectangular columnar phase at 150 °C, the smallest BTA (**C6**) still showed a weakly birefringent texture under POM after the field had been turned on for 15 min, indicating imperfect homeotropic alignment. Complete perpendicular alignment could only be achieved readily at 170 °C in the hexagonal columnar phase by applying a larger electric field of 34 V/μm for about 10 min.

The alignment in the BTAs is remarkably slow when compared to the switching time in the order of 1 ms reported by Bushey et al. for a hexagonal columnar LC phase of a structurally very similar crowded BTA under nearly equal experimental conditions (160 °C, 15–20 V/μm).[36] In line with the slow alignment process and in contrast with the results of Bushey, however, the aligned state is stable in the absence of an electric field for all three BTAs. Upon cooling the aligned samples, the texture of **C10** remains virtually black under POM for days, indicating that the homeotropic alignment of the columns is preserved at room temperature. As can be expected on the basis of the DSC results, a birefringent texture is formed for **C6** and **C18** at lower temperatures as a result of crystallization. Interestingly, we found earlier that the black texture for **C18** reappears upon cooling after the sample has been heated above the melting point of the crystalline phase without a field across the cell. This indicates that the basic columnar structure and its alignment are unaffected by the crystallization process for this BTA.[15]

2.2.2. Polar Switching in the LC Phase. The ferroelectric behavior of the BTAs was initially characterized by measuring the current response induced by the polar switching process.[3,37,38] For these switching experiments, previously aligned samples were cooled to the desired measurement temperature and preservation

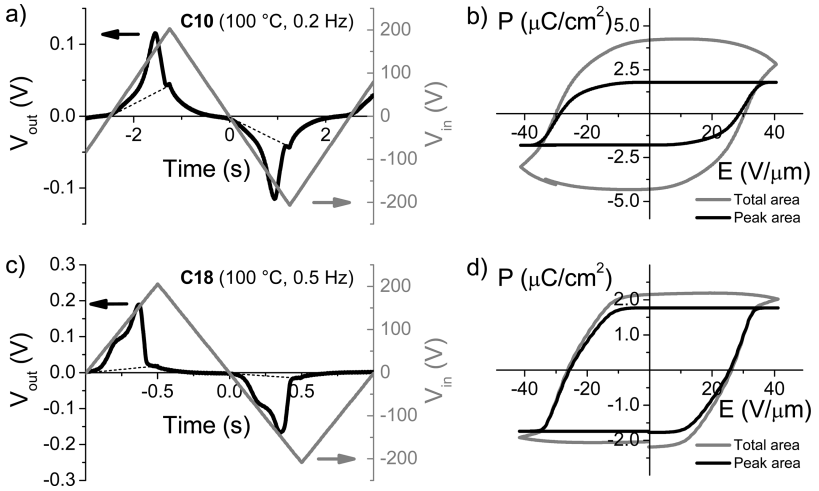

Figure 2. Results of the polar switching experiments under a triangular wave input voltage for **C10** (top, a and b) and **C18** (bottom, c and d) at 100 °C. (a,c) The input voltage (dark gray, right axis) and the voltage over the measurement resistance resulting from the polarization current as function of time (black, left axis). Measurement conditions are noted on the top right and the baseline used for integration of the current peak is indicated by the dotted lines. (b,d) Polarization against field (P–E hysteresis loops) calculated from the data in (a) and (c), respectively. The polarization evaluated based on the total area under measured voltage curves is plotted in dark gray, and the polarization based solely on the area of the peak is plotted in black.

dx.doi.org/10.1021/jp300008f | J. Phys. Chem. B 2012, 116, 3928–3937

Table 2. Results of Polar Switching Measurements under Triangular Wave Input Voltage

	P_s, μC/cm^2[a]		E_c, V/μm[a]		f_{max}, Hz[b]	
T, °C	C10	C18	C10	*CX18*	C10	C18
70	NA[c]	1.6 ± 0.2	NA	25.8 ± 0.3	NA	0.1
100	1.8 ± 0.3	1.7 ± 0.1	29.2 ± 1.9	25.2 ± 0.9	0.2	0.5
120	1.5 ± 0.3	1.6 ± 0.1	28.1 ± 1.7	23.1 ± 1.5	0.6	1.0
150	1.6 ± 0.3	1.4 ± 0.1	26.6 ± 2.3	21.0 ± 1.1	3.0	5.0

[a]Values are averaged over at least three measurements from at least two unique cells. The reported error margin is the standard deviation of the measured values. [b]Maximum driving frequency that allowed the polarization to saturate at the given temperature. All measurements were conducted at or slightly below this frequency. [c]The polarization did not saturate completely at this temperature, even at the lowest measurement frequency (0.1 Hz).

of the perpendicular alignment was checked by POM. Next, a triangular wave voltage was applied (0.1−5 Hz, 400 $V_{p\text{-}p}$) and the current response of the cell was monitored by measuring the voltage over a 10 kΩ resistance in series with the measurement cell. The input signal and the voltage response of the cell were recorded simultaneously by a digital oscilloscope. One full cycle of such a polar switching experiment for **C10** and **C18** at 100 °C is depicted in Figure 2a,c. The area of the peak is plotted in black.

Unfortunately, none of the samples prepared for **C6** allowed a full set of switching experiments due to short circuits in the measurement cells. The cell response curves for both **C10** and **C18** are dominated by two voltage peaks with an opposite sign that are symmetric in the *x*-axis and match the sign of the applied field. Two important features of the cell response peaks should be noted. First, the onset of the peaks clearly occurs after the applied field has passed 0 V, consistent with ferroelectric behavior. Second, the signal returns to the slightly curved baseline before the input voltage ramp reaches its maximum value, proving that reversal of the polarization is completely saturated under these experimental conditions. The background signal in the switching experiment is much more pronounced for the **C10** samples than for **C18**. In both cases, we ascribed the baseline signal to some residual conductance related to ionic impurities in the samples and the geometric capacitance of the LC cell. The polarization reversal peaks are not completely symmetric, especially in the case of **C18**, pointing to an inhomogeneous switching process. Finally, it is worth mentioning that the initial black POM textures of both BTAs remain unchanged throughout the switching process.

To determine the spontaneous polarization (P_s) and coercive field (E_c) that characterize the polar switching process in the BTAs, the observed polarization was plotted as a function of the applied electric field (Figure 2b,d). These *P*−*E* loops were constructed by integrating the cell response voltage as a function of time and using the known values of the measurement resistance, cell spacing, and electrode area.[39] When the total area under the cell response curves is used for this procedure, a total polarization is obtained that contains contributions from both the polarization of the polar switching process as well as the conductive and capacitive effects (gray lines in Figure 2b,d). The *P*−*E* loops show clear hysteresis as well as a concave and fairly symmetric shape indicative of polar switching. Nonetheless, the *P*−*E* loops also have a convex region that is typical for a imperfect or lossy dielectric material exhibiting conductance.[40] As expected, the lossy character of the samples makes a significant contribution to the total current through the circuit and, thus, to the calculated polarization, especially in the case of **C10**. Therefore, the values for the coercive field and residual polarization were estimated based on the area of the voltage peak due to polarization reversal by assuming a linear baseline under this peak (black lines in Figure 2b and d, baseline indicated by dotted lines in Figure 2a,c). The parameters P_s and E_c were determined from the axis crossings of the *P*−*E* loops obtained in this manner and resulted in values of 25−30 V/μm and 1−2 μC/cm^2, respectively, for both BTAs.

Analogous measurements were performed for multiple samples at several temperatures in the columnar LC phase of **C10** and **C18**. During these experiments the frequency of the triangular wave voltage was adjusted to allow the polarization to saturate completely. All measurements were conducted at or slightly below the maximal switching frequency (f_{max}), and *P*−*E* loops were constructed as described above to determine the ferroelectric parameters. The average spontaneous polarization, coercive field, and the maximal attainable switching frequency for the different experimental conditions are collected in Table 2.

In general, there is a significant spread in the experimental values for the spontaneous polarization, while the reproducibility of the coercive fields is far better. We attribute the larger experimental error in the polarization values mainly to the unavoidable presence of small air bubbles in the electrode area that were observed by POM in most of the samples. The average P_s values for both BTAs vary between 1.4 and 1.8 μC/cm^2 and do not differ much over the 70−150 °C temperature range. The coercive fields decrease with increasing temperature and are somewhat lower for **C18** than for **C10**, indicating that switching is somewhat easier in the former compound. In line with the trend in E_c values, the maximum switching speed for both compounds increases significantly over the same temperature interval with **C18** displaying somewhat faster polarization reversal.

The spontaneous polarization of the BTAs is almost 1 order of magnitude higher compared to the two main literature examples of switchable columnar phases with axial polarity (70−600 nC/cm^2)[3,9,41,42] and typical values reported for ferroelectric smectic and columnar LC phases (50−500 nC/cm^2).[4,7,38,43,44] Moreover, both the coercive field and the spontaneous polarization are very much comparable to the well-known organic ferroelectric poly(vinylidene fluoride) (PVDF, E_c = 50 V/μm and P_s = 8 μC/cm^2).[45,46] The maximum switching frequencies fall slightly below the range reported for comparable columnar LC phases (up to 18 Hz), but are far lower than for PVDF, which can easily reach switching speeds in the kHz range.[3,9,47]

The switching behavior of the BTAs exhibits the hallmarks of a ferroelectric material, namely a single switching peak every half-period of the triangular wave input signal with a delayed onset with respect to the applied field. However, as has been pointed out in studies by Haase and Kishikawa, ionic and charge relaxation phenomena can give rise to comparable switching behavior at sufficiently low frequencies.[3,37,48] Therefore, these

dx.doi.org/10.1021/jp300008f | J. Phys. Chem. B 2012, 116, 3928−3937

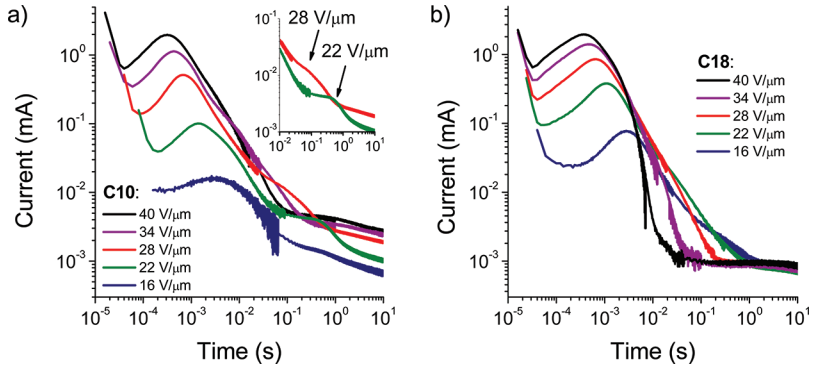

Figure 3. Cell response currents after field reversal for selected values of the electric field. The current was measured over a 10 kΩ resistance under application of a low-frequency rectangular wave input voltage. (a) For **C10**. The curves at 28 and 22 V/μm clearly show the presence of second current peak (inset). (b) For **C18**.

authors have stated that it is important to consider the dependence of the polarization on temperature and switching frequency. The constant value of the spontaneous polarization for both BTAs, even at relatively low frequencies at 150 °C, strongly indicates that the switching process indeed originates from the polar character of the BTA columns.

Alternatively, the absolute value of the spontaneous polarization provides additional evidence for the origin of the switching behavior. The polarization mechanism we propose implies that all BTA columns are aligned and poled uniformly at the highest field in the triangular wave experiments and that the observed switching corresponds to a complete reversal of the orientation of the macrodipoles. Under these assumptions, we can simplify the general equation defining the spontaneous polarization in the following manner[43]

$$P_s = \frac{1}{V}\sum_{i}^{N} \mu_i = \frac{1}{V_m}\mu \qquad (1)$$

where V_m is the molecular volume of the BTA in the hexagonal columnar phase and μ is the total effective dipole moment of the three amide bonds in each BTA. Entering the known molecular volume of the BTAs at 150 °C from the WAXS results and the polarization values from Table 2 in eq 1 leads to a calculated dipole moments of 5.8 and 8.3 D for **C10** and **C18**, respectively. These values are in excellent agreement with the average dipole moments calculated for stacked BTAs in several molecular modeling studies (6−14 D).[23,30,49]

2.2.3. Characterization of the Switching Process: Extrinsic Switching. There are two general mechanisms via which the polarization switching process in a ferroelectric can occur. In an ideal ferroelectric, the dipoles in the system are perfectly correlated and they switch either coherently or not at all. This process does not involve a nucleation step and is therefore called intrinsic switching. The alternative mechanism, referred to as nucleated or extrinsic polarization switching, is almost invariably observed for all real ferroelectric materials.[50−52] The overall speed of polarization reversal in the extrinsic switching process is determined by the interplay between the nucleation of domains with opposite polarity and their subsequent growth.[53]

To further confirm the dipolar origin of the polarization reversal and to characterize the nature of the switching process, switching experiments were performed by applying a low-frequency rectangular wave over the sample cells with variable input voltages (0.1−1.0 Hz, 160−400 V_{p-p}). The cell response current was captured in two separate time frames to monitor both the fast and slow processes occurring after inversion of the applied field. The combined data of the current response directly after field inversion for **C10** and **C18** are plotted on a double-logarithmic scale in Figure 3a,b for selected field strengths.

The transient current response for both BTAs exhibits the same general characteristics. The initial response of the cells up to approximately 10^{-4} s shows a rapid exponential decrease of the current typical for an RC circuit. In the range of 10^{-4}−10^{-1} s, the transient current is dominated by a broad peak attributed to the polar switching process in the BTAs. The top of these switching peaks shifts to longer times and the peaks fall off more slowly with decreasing field strength. At very long times (10 s), the transient current drops to an approximately constant value that scales linearly with the applied electric field. We attribute this feature to ohmic conduction in the samples.[54] The fact that the conduction-related current at long times is higher for **C10** than for **C18** samples is consistent with the results obtained earlier for the switching experiments with a triangular wave voltage. Another difference between the two BTAs is the appearance of a second switching peak at longer times and lower fields for **C10** (see inset in Figure 3a). At higher fields the two switching peaks coincide, whereas the second peak is not detectable for fields below 20 V/μm, indicating that the switching event associated with the second peak slows down much more strongly with decreasing electric field than the reversal of the macrodipole. Therefore, we assign the second switching event to an ionic or charge relaxation process that is strongly activated by the electric field.

The observation of a field-dependent peak in the transient current originating from the polar switching process in **C10** and **C18** is typical for a nucleated or extrinsic polarization switching process.[50] At high field strengths, the nucleation is very fast and the speed of the switching process is dominated by the domain growth. Under these high-field conditions, a single power law dependence is expected between the switching time and the applied field.[55−58] Taking the time for the switching peak to reach its maximum current (t_p) as a measure for the switching time, the expected linear relation between switching time and electric field on a double-logarithmic scale is observed for both BTAs (Figure 4). In line with the results presented earlier in Table 2, the graph in Figure 4 shows clearly that the switching speeds for **C10** and **C18** are similar and become faster with increasing temperature. In addition, the maximum polarization values obtained by integrating the cell response curves in Figure 4 are in good agreement with the spontaneous polarization determined from the triangular wave experiments.[59]

dx.doi.org/10.1021/jp300008f | J. Phys. Chem. B 2012, 116, 3928−3937

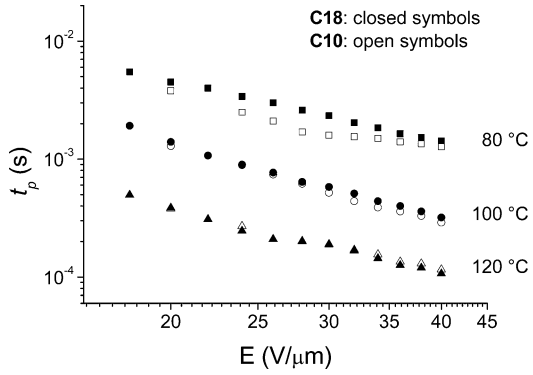

Figure 4. Switching time (time of the top of the switching peak, t_p) for **C10** and **C18** as function of electric field at 80, 100, and 120 °C (double-logarithmic scale).

Although these results clearly indicate that the switching process in the BTAs is extrinsic, it is unclear whether domain growth occurs predominantly along the column axis, in the plane of the hexagonal columnar lattice, or simultaneously along both directions. Finally, it should be noted that extrinsic switching is inherently an inhomogeneous process that can be initiated by defects in the phase structure or small amounts of impurities. Therefore, the asymmetric peak shapes obtained during some of the triangular wave measurements can well be explained by the extrinsic nature of the switching mechanism.

2.2.4. Depolarization in the LC Phase. Apart from being switchable, the strict definition of a ferroelectric material requires the polarized state to be stable in the absence of an external field.[46] To investigate whether the columnar LC phase in BTAs is properly ferroelectric, the lifetime of the polarized state was measured using the experiment depicted schematically in Figure 5a. After an initial long pulse ($E > E_c$) in which the columns are poled uniformly, the field is removed for a period of time (t_r) to allow the polarization to relax. Subsequently, a pulse is given with either negative or positive polarity and the transient current response of the cell is measured. If the spontaneous polarization is stable during t_r, a positive pulse will not change the polarization of the samples, while the negative pulse will lead to polarization reversal accompanied by a current response peak. In this case, the total integral under the response peak for the negative pulse will equal $2P_s$ as noted previously. Correspondingly, if the original polarization is completely relaxed during t_r, both the positive and negative pulse will lead to a buildup of polarization (with a opposite polarity) and the integrated response signal will equal P_s in both cases. Figure 5b shows the results of such a measurement for different time intervals t_r for **C18** at 140 °C. Indeed, the signals resulting from positive and negative pulses converge rapidly from their starting values (0 and $2P_s$, respectively) to the value of P_s with increasing relaxation time. In this measurement, it takes about 0.5 s for the spontaneous polarization to drop to half its initial value.

Similar experiments were performed using only positive pulses for both **C10** and **C18** at different temperatures. Fortunately, the secondary polarization process in **C10** did not appear in these positive pulse measurements. This observation indicates that the corresponding polarization relaxes very slowly in the absence of an electric field and corroborates the earlier assignment of this second polarization process to a strongly field-activated process. The absence of the secondary polarization process allowed us to accurately determine the polarization arising from **C10**. Figure 6a shows the normalized remaining polarization $1 - (P_r/P_s)$ as a function of t_r for **C10** and **C18** at four different temperatures.

The half-life of the spontaneous polarization for both BTAs increases strongly with decreasing temperature to a maximum value of ~50 s at 80 °C. Most importantly, these results prove that at least in these devices the spontaneous polarization in the BTAs has a finite lifetime, suggesting that the columnar LC phases are strictly speaking not ferroelectric. We will come back to this at the end of this section. The increase of the depolarization time with decreasing temperature matches the trend observed earlier for the maximum switching frequency and the switching time, although depolarization proceeds significantly slower than the field-induced switching. For comparison, the time scale on which depolarization takes place for the urea-based polar columnar LC system studied by Kishikawa and co-workers is 10 ms at 160 °C, about an order of magnitude faster than for the BTAs studied here.[10−12]

To quantitatively characterize the time dependence of the depolarization, the data sets in Figure 6a were fitted to a stretched exponential function

$$1 - \frac{P(t_r)}{P_s} = \exp\left(-\left(\frac{t_r}{\tau}\right)^{\beta}\right) \quad (2)$$

where τ is the characteristic relaxation time of the process and β is the stretching parameter ($\beta < 1$). Such functions are

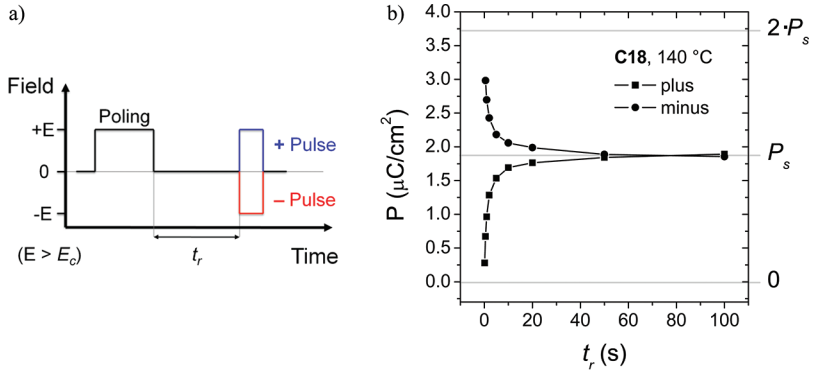

Figure 5. (a) Schematic representation of input pulses for the polarization lifetime experiments. (b) Total polarization (integrated current response) measured by the pulses defined in (a) as a function of the relaxation time (t_r) in a lifetime experiment for **C18** (140 °C). Lines connecting the data points serve to guide the eye.

dx.doi.org/10.1021/jp300008f | J. Phys. Chem. B 2012, 116, 3928−3937

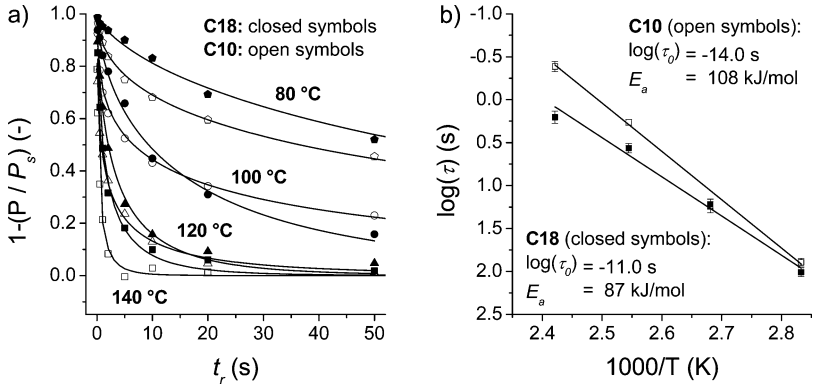

Figure 6. Results of the temperature-dependent lifetime experiments for **C10** and **C18**. (a) Normalized remaining polarization as a function of the relaxation time (t_r). The lines represent a stretched exponential fit to the data sets (β = 0.4–0.6). (b) Activation plot for the depolarization process in **C10** and **C18**. The error bars correspond to the standard deviations from the stretched exponential fits in (a). The lines result from a fit of the data points to Arrhenius' law. The corresponding activation parameters are reported on the top right (**C10**) and bottom left (**C18**).

commonly used to describe the time dependence of processes that are characterized by a distribution in relaxation times, such as glass transitions.[60−62] As can be seen in Figure 6a, eq 2 describes the depolarization process in the BTAs very well with β values between 0.4 and 0.6. By further assuming Arrhenius behavior for the temperature dependence of the relaxation time, a quantitative estimate of the characteristic activation parameters of the depolarization process was made (Figure 6b). The activation energy values that follow from this analysis are 108 and 87 kJ/mol for **C10** and **C18**, respectively.

The question remains why the material depolarizes under zero applied field. Potentially, this can be related to the used ITO electrodes. It is well established that strong depolarization fields arise when the polarization charge on the dielectric surface is not compensated by counter charges in the electrodes.[63−65] Since ITO is a (heavily doped) n-type semiconductor, it might not properly stabilize negative polarization charges, causing fast depolarization. In order to rule out this option, we made devices using Au electrodes. The results are described in detail in the Supporting Information. In brief, we find that use of Au electrodes significantly slows down the depolarization but does not prevent it. The depolarization mechanism appears to be independent of electrode material. Hence, the ground state of these layers is not a polarized unidomain. Various structural models have been proposed in the literature for the unpolarized state in systems with hexagonal symmetry based on theoretical[66−68] and, recently, experimental[11,69] studies. The precise nature of the unpolarized ground state in case of BTAs remains unclear and is a topic of further research.

2.3. Dielectric Relaxation Spectroscopy. DRS is a spectroscopic technique that probes the interaction of electromagnetic waves with matter in the frequency regime between 10^{-6} and 10^{12} Hz. The dielectric dispersions and absorptions in solid insulating materials and polar liquids that occur in this frequency range are generally referred to as dielectric relaxations and can be linked to reorientational motions of molecular dipoles and charge transport in such materials.[70] By collecting dielectric spectra in a wide temperature range the thermodynamic parameters governing the dynamics of these relaxation processes can be determined. Therefore, investigation of the dipolar relaxations in BTAs by means of DRS is ideally suited to gain more insight in both the dynamic nature of the columnar LC phases and the molecular processes that are responsible for the observed polar switching behavior.

DRS measurements were performed between −140 and 250 °C upon cooling from the isotropic melt in a frequency range from 10^{-1} to 10^{6} Hz. The complete dielectric spectrum recorded for **C10** is shown in Figure 7. For each BTA, one or

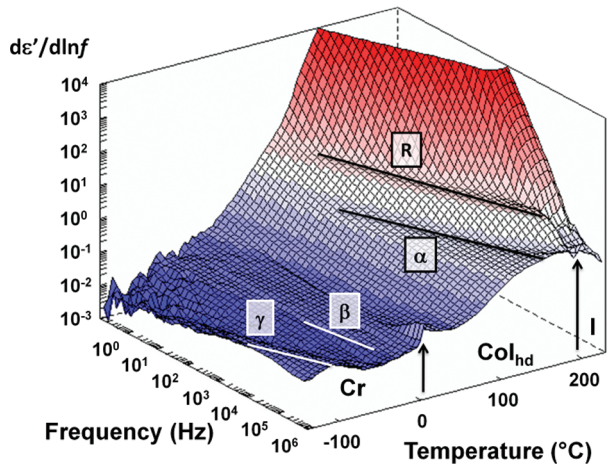

Figure 7. Dielectric spectrum for **C10**. The dielectric loss is plotted as dε′/d ln f according to ref 71. All dielectric relaxation processes are marked by lines and labeled as in Table 3. The phase transitions are indicated by arrows and the phases are labeled above the temperature axis.

two relaxation processes can be observed in the crystalline phase (γ and β) below room temperature and two more relaxation processes are present at higher temperatures in the columnar LC phase (α and R). Characteristic relaxation times and thermal activation parameters (Arrhenius behavior) were determined for each of the relaxation processes using a fitting procedure described elsewhere.[71] Additionally, the activation enthalpy and entropy for all processes were computed from the Arrhenius parameters using the Starkweather analysis.[72,73] Since we are primarily interested in the molecular origin of the ferroelectric behavior of the BTAs, only the relaxation processes occurring in the LC phase where switching is observed will be discussed in detail in the following subsections.

2.3.1. Low-Temperature Relaxation Process in the LC Phase: a Columnar Glass Transition. The dielectric spectra for

dx.doi.org/10.1021/jp300008f | J. Phys. Chem. B 2012, 116, 3928−3937

Table 3. Activation Parameters for the α- and R-Relaxation Processes in the BTAs

process	BTA	log(τ_0), s	E_a, kJ mol^{-1}[a]	ΔH, kJ mol^{-1}[b]	ΔS, J mol^{-1} K^{-1}[b]	T_g, °C (m, −)[c]
α	**C6**	−11.6	13			41 (88)
	C10	−13.3	23			50 (64)
	C18	−11.7	21			54 (56)
R	**C6**	−21.3	138	84	153	
	C10	−22.1	147	86	168	
	C18	−19.1	124	85	111	

[a]The value reported for the α-process is the Vogel−Fulcher−Tammann activation energy (E_v). [b]Calculated based on the Starkweather analysis.[72] [c]The glass transition temperature is reported as the temperature where τ_α = 100 s. The steepness index (m) as defined in the main text is reported between parentheses.

all three BTAs reveal an α-relaxation in the low-temperature range of the LC phase. The temperature dependence of the relaxation time (τ) of the α-relaxations is not Arrhenius-like and can be described by the Vogel−Fulcher−Tammann (VFT) equation

$$\tau = \tau_0 \exp\left(\frac{E_v}{R(T - T_v)}\right) \quad (3)$$

where E_v and T_v are the Vogel activation energy and Vogel temperature and the other parameters (R, τ_0) have their standard meanings.[74] The VFT equation is a generally accepted relation that describes the temperature dependence of the structural relaxation time or viscosity of supercooled (glass-forming) liquids above the glass transition very well. Based on the VFT parameters, it is convenient to define the operational glass transition temperature (T_g) as the temperature at which τ equals 100 s.[75] For the BTAs investigated here, the glass transition temperature ranges from 41 to 54 °C. Apparently, the molecular motions involved in the α-relaxation start slowing down in a temperature region where the BTAs are in the LC phase and the alkyl side chains attached to the core are still highly mobile. Consequently, the α-relaxation must be associated with freezing of certain molecular motions within the columnar structure of the LC phase.

Glass transitions with similar characteristics have been reported in the literature for columnar LC and columnar plastic mesophases formed by discotics with hexabenzocoronene and triphenylene cores.[61,74,76,77] A parameter that can be used to classify different glass-forming compounds is the steepness or fragility index (m) defined as

$$m = \left.\frac{\mathrm{d}\log(\tau)}{\mathrm{d}(T_g/T)}\right|_{T=T_g} = \frac{E_v}{2.303R}\frac{T_g}{(T_g - T_v)^2} \quad (4)$$

The value of the steepness index has theoretical limits of 16 and 200 for so-called ideal *strong* and *fragile* glass-formers, respectively, and is a measure for how progressively the degree of cooperativity of the dynamic glass transition evolves toward the glass transition temperature.[61,74] Apart from the specific interactions occurring in the system, the steepness index is related to the dimensionality of the network that allows the growth of the cooperativity volume near the glass transition temperature. The steepness indices that were determined from the dielectric spectra of the BTAs are between 54 and 88. The rather low values for m are in good agreement with the results obtained for columnar glass transitions in a number of triphenylene discotics forming hexagonal LC phases and favor the idea that the α-relaxation in BTAs is predominantly an intracolumnar process.[61]

Based on extensive solid-state NMR studies, the α-processes in columnar mesophases formed by hexabenzocoronene- and triphenylene-based discotics have been attributed to collective rotations of the discotics around the columnar axis.[76−78] However, the individual discotics or column segments in the BTA columns would have to break six hydrogen bonds to neighboring molecules in the column in order to rotate, whereas these discotics are mainly held together by favorable π−π interactions that remain intact during rotational motions. Such a molecular picture is not consistent with the rather low activation energy of the α-process and makes a similar assignment highly unlikely. As an alternative, we propose that the hydrogen bonds are dynamic enough to allow for collective vibrations of the BTAs along the column axis in the LC phase that give rise to significant dielectric relaxations. The cooperative vibration of discotics will locally unwind the helical structure somewhat, leading to straighter alignment of the amide bonds with respect to the column axis and a stronger macrodipole. The orientation of the macrodipole is not changed during this unwinding process, suggesting that the α-process is not connected to the polar switching of BTAs.

Solid-state ^{1}H NMR spectra were recorded around the glass transition temperature (30−120 °C) for C10 to corroborate the abrupt change in mobility that is expected in this temperature range based on the DRS study.[79] The NMR results clearly show a much higher mobility for the side chains compared to the hydrogen-bonded core regions as well as an abrupt change in the overall dynamics of the BTAs around 50−70 °C. These observations further support the assignment of the α-process to collective vibrations in the hydrogen-bonded columns that freeze out at ambient temperatures below the glass transition temperature (Figure 8).

2.3.2. High-Temperature Relaxation Process in the LC Phase: Reorientational Dynamics of the Macrodipole. In the high-temperature region (~120−200 °C) of the LC phase, the much slower R-relaxation process is observed in the dielectric relaxation spectra for all three BTAs. The dielectric spectrum for **C6** in this region does not exhibit a discontinuity at the transition from the Col_{rd} to the Col_{hd} phase, showing that the R-relaxation is not influenced by the slight change in the LC structure. The thermal activation of this process obeys the Arrhenius equation and is characterized by a substantial activation energy (124−138 kJ/mol). Moreover, the calculated activation entropy for the R-relaxation is very high (111−168 J/(mol·K)), indicating that this process is associated with strongly cooperative molecular motions involving larger length scales.

Slow and cooperative processes at higher temperatures have been reported earlier for columnar mesophases in hexabenzocoronene derivatives and vanadyl complexes. In these studies, the slow relaxation processes were assigned to collective reorientations of whole (short) columns and, respectively, to

dx.doi.org/10.1021/jp300008f | J. Phys. Chem. B 2012, 116, 3928−3937

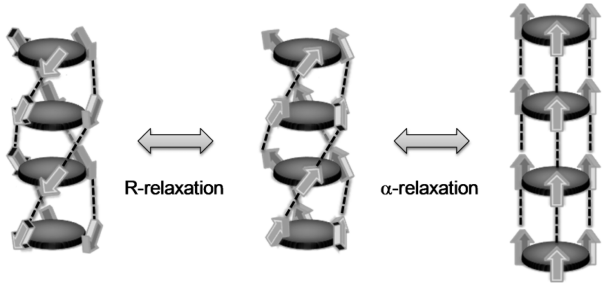

Figure 8. Schematic overview of the assignment for the α- and R-relaxation processes in BTAs uncovered in the DRS study. The BTA core is depicted as a dark gray disk and the amide groups as light gray arrows indicating the orientation of the dipole moment (side chains are omitted for clarity). Hydrogen bonds between the amide groups are shown as dotted black and gray lines.

collective 180° reorientational jumps of polar groups within the columnar structure.[37,77] Given the structural similarity between the LC phases formed by the polar vanadyl complexes and the hydrogen-bonded columnar LC phase of the BTAs, we ascribe the R-process to the latter relaxation mode, although a conclusive assignment is not possible solely based on the dielectric relaxation data (Figure 8).

It is important to realize that the collective reorientation of amide groups in BTAs corresponds to inversion of the macrodipole over a certain length along the columns. Therefore, the presence of the R-process might well explain the polar switching of BTAs reported earlier and described in the previous section.[15,32−34] Moreover, there is a striking agreement between the activation energies associated with the R-relaxation in the DRS study and the depolarization process (see Figure 6b, 108 and 87 kJ/mol). The match in activation energies strongly suggests that the molecular mechanism for both processes is identical and involves the cooperative rotation of amides along the column axis. However, the absolute time scale of the two processes at a given temperature, as determined by the pre-exponential factor in the Arrhenius equation, differs over 3 orders of magnitude. We propose that the R-relaxation is considerably faster mainly because DRS probes the inversion of the macrodipole locally over small sections of the columns. In contrast, the slower depolarization process takes place over macroscopic distances requiring nucleation and subsequent growth of domains with an opposite polarity.

3. CONCLUSIONS

Polar switching in three BTAs with different alkyl chain lengths (**C6**, **C10**, and **C18**) has been investigated. Due to the presence of a macrodipole, the hexagonal columnar LC phase of all three BTAs can be aligned uniformly in LC cells with a spacing of 5 μm by applying a dc field in the order of 30 V/μm. Moreover, temperature-dependent switching experiments showed that **C10** and **C18** display extrinsic polar switching characterized by a spontaneous polarization and coercive field of 1−2 μC/cm^2 and 20−30 V/μm, respectively. The value of the spontaneous polarization is in line with the expected value based on the effective dipole moment of BTAs in columnar stacks reported in the literature and is fairly constant between 70 and 150 °C, supporting the assignment of the polar switching process to complete inversion of the macrodipoles in the BTA columns. In the absence of an external field, the spontaneous polarization for both **C10** and **C18** is lost in 1−1000 s depending on temperature and device details. Hence, the ground state of the columnar LC phases of BTAs is not a polarized monodomain.

The DRS study revealed an α-process that is associated with collective vibrations in the hydrogen-bonded columns that freeze out at ambient temperatures under the glass transition temperature (41−54 °C). In the high-temperature region (∼120−200 °C) of the LC phase, the much slower R-relaxation process is observed for all three BTAs. This relaxation process is assigned to the collective reorientation of amide groups in the BTAs and corresponds to an inversion of the macrodipole along the column axis. Matching activation energies suggest that the molecular mechanism underlying the R-processes is also responsible for the polar switching process. In general, the results presented here underline that LC phases based on BTAs offer the unique possibility to integrate polarization with other functionalities in a single nanostructured material.

■ ASSOCIATED CONTENT

Supporting Information

Experimental section; X-ray scattering data of **C6**, **C10**, and **C18**; ohmic conduction of C10 and C18 LC cells; determination of the total polarization in the rectangular wave experiments; DRS relaxation processes in the crystalline phase; solid-state ^{1}H NMR data for **C10**; and depolarization behavior between Au electrodes. This material is available free of charge via the Internet at http://pubs.acs.org.

■ AUTHOR INFORMATION

Corresponding Author

*E-mail: r.p.sijbesma@tue.nl.

Notes

The authors declare no competing financial interest.

■ ACKNOWLEDGMENTS

The authors thank Prof. Dago de Leeuw and Dr. Kamal Asadi of the University of Groningen for stimulating discussions. Ben Norder and Dr. Eduardo Mendes of the Technical University of Delft are acknowledged for providing access to their WAXS setup. The authors further thank Mr. Brahim Mezari for his assistance with the solid-state NMR experiments. This work has been financially supported by The Netherlands Organization for Scientific Research, Chemical Sciences (NWO-CW).

■ REFERENCES

(1) Asadi, K.; De Leeuw, D. M.; De Boer, B.; Blom, P. W. M. *Nat. Mater.* **2008**, *7*, 547−550.
(2) Naber, R. C. G.; Asadi, K.; Blom, P. W. M.; De Leeuw, D. M.; De Boer, B. *Adv. Mater.* **2009**, *22*, 933−945.
(3) Kishikawa, K.; Nakahara, S.; Nishikawa, Y.; Kohmoto, S.; Yamamoto, M. *J. Am. Chem. Soc.* **2005**, *127*, 2565−2571.
(4) Bock, H.; Helfrich, W. *Liq. Cryst.* **1995**, *18*, 707−713.
(5) Lagerwall, J. P. F; Giesselmann, F. *ChemPhysChem* **2006**, *7*, 20−45.
(6) Lagerwall, S. T. In *Handbook of Liquid Crystals, Vol. 2b, Low Molecular Weight Liquid Crystals II*; Demus, D., Goodby, J., Gray, G. W., Spiess, H.-W., Vill, V., Eds.; Wiley-VCH: Weinheim, Germany, 1998; pp 515−664.
(7) Scherowsky, G.; Chen, X. H. *J. Mater. Chem.* **1995**, *5*, 417−421.
(8) Takezoe, H.; Kishikawa, K.; Gorecka, E. *J. Mater. Chem.* **2006**, *16*, 2412−2416.
(9) Gorecka, E.; Pociecha, D.; Mieczkowski, J.; Matraszek, J.; Guillon, D.; Donnio, B. *J. Am. Chem. Soc.* **2004**, *126*, 15946−15947.
(10) Gorecka, E.; Pociecha, D.; Matraszek, J.; Mieczkowski, J.; Shimbo, Y.; Takanishi, Y.; Takezoe, H. *Phys. Rev. E* **2006**, *73*, 031704.
(11) Okada, Y.; Matsumoto, S.; Araoka, F.; Goto, M.; Takanishi, Y.; Ishikawa, K.; Nakahara, S.; Kishikawa, K.; Takezoe, H. *Phys. Rev. E* **2007**, *76*, 041701.

(12) Okada, Y.; Matsumoto, S.; Takanishi, Y.; Ishikawa, K.; Nakahara, S.; Kishikawa, K.; Takezoe, H. *Phys. Rev. E* **2005**, *72*, 020701.
(13) (a) Miyajima, D.; Araoka, F.; Takezoe, H.; Kim, J.; Kato, K.; Takata, M.; Aida, T. *J. Am. Chem. Soc.* **2010**, *132*, 8530−8531. (b) Miyajima, D.; Araoka, F.; Takezoe, H.; Kim, J.; Kato, K.; Takata, M.; Aida, T. *Angew. Chem., Int. Ed.* **2011**, *50*, 7865−7869.
(14) Fitié, C. F. C.; Mendes, E.; Hempenius, M. A.; Sijbesma, R. P. *Macromolecules* **2011**, *44*, 757−766.
(15) Fitié, C. F. C.; Roelofs, W. S. C.; Kemerink, M.; Sijbesma, R. P. *J. Am. Chem. Soc.* **2010**, *132*, 6892−6893.
(16) Fitié, C. F. C.; Tomatsu, I.; Byelov, D.; De Jeu, W. H.; Sijbesma, R. P. *Chem. Mater.* **2008**, *20*, 2394−2404.
(17) Matsunaga, Y.; Miyajima, N.; Nakayasu, Y.; Sakai, S.; Yonenaga, M. *Bull. Chem. Soc. Jpn.* **1988**, *61*, 207−210.
(18) Matsunaga, Y.; Nakayasu, Y.; Sakai, S.; Yonenaga, M. *Mol. Cryst. Liq. Cryst.* **1986**, *141*, 327−333.
(19) Bose, P. P.; Drew, M. G. B.; Das, A. K.; Banerjee, A. *Chem. Commun.* **2006**, 3196−3198.
(20) Lightfoot, M. P.; Mair, F. S.; Pritchard, R. G.; Warren, J. E. *Chem. Commun.* **1999**, 1945−1946.
(21) Ranganathan, D.; Kurur, S.; Gilardi, R.; Karle, I. L. *Biopolymers* **2000**, *54*, 289−295.
(22) Sakamoto, A.; Ogata, D.; Shikata, T.; Urakawa, O.; Hanabusa, K. *Polymer* **2006**, *47*, 956−960.
(23) Shikata, T.; Kuruma, Y.; Sakamoto, A.; Hanabusa, K. *J. Phys. Chem. B* **2008**, *112*, 16393−16402.
(24) Yasuda, Y.; Iishi, E.; Inada, H.; Shirota, Y. *Chem. Lett.* **1996**, 575−576.
(25) Zhou, Y. F.; Xu, M.; Wu, J. C.; Yi, T.; Han, J. T.; Xiao, S. Z.; Li, F. Y.; Huang, C. H. *J. Phys. Org. Chem.* **2008**, *21*, 338−343.
(26) Brunsveld, L.; Schenning, A. P. H. J.; Broeren, M. A. C.; Janssen, H. M.; Vekemans, J. A. J. M.; Meijer, E. W. *Chem. Lett.* **2000**, 292−293.
(27) Smulders, M. M. J.; Buffeteau, T.; Cavagnat, D.; Wolffs, M.; Schenning, A. P. H. J.; Meijer, E. W. *Chirality* **2008**, *20*, 1016−1022.
(28) Smulders, M. M. J.; Schenning, A. P. H. J.; Meijer, E. W. *J. Am. Chem. Soc.* **2008**, *130*, 606−611.
(29) Filot, I. A. W.; Palmans, A. R. A.; Hilbers, P. A. J.; Van Santen, R. A.; Pidko, E. A.; De Greef, T. F. A. *J. Phys. Chem. B* **2010**, *114*, 13667−13674.
(30) Stals, P. J. M.; Everts, J. C.; De Bruijn, R.; Filot, I. A. W.; Smulders, M. M. J.; Martin-Rapun, R.; Pidko, E. A.; De Greef, T. F. A.; Palmans, A. R. A.; Meijer, E. W. *Chem.--Eur. J.* **2010**, *16*, 810−821.
(31) Stals, P. J. M.; Smulders, M. M. J.; Martin-Rapun, R.; Palmans, A. R. A.; Meijer, E. W. *Chem.—Eur. J.* **2009**, *15*, 2071−2080.
(32) Sugita, A.; Suzuki, K.; Kubono, A.; Tasaka, S. *Jpn. J. Appl. Phys.* **2008**, *47*, 1355−1358.
(33) Sugita, A.; Suzuki, K.; Tasaka, S. *Chem. Phys. Lett.* **2004**, *396*, 131−135.
(34) Sugita, A.; Suzuki, K.; Tasaka, S. *Jpn. J. Appl. Phys.* **2008**, *47*, 8043−8048.
(35) See Supporting Information.
(36) Bushey, M. L.; Nguyen, T. Q.; Nuckolls, C. *J. Am. Chem. Soc.* **2003**, *125*, 8264−8269.
(37) Kilian, D.; Knawby, D.; Athanassopoulou, M. A.; Trzaska, S. T.; Swager, T. M.; Wrobel, S.; Haase, W. *Liq. Cryst.* **2000**, *27*, 509−521.
(38) Yelamaggad, C. V.; Shanker, G.; Rao, R. V. R.; Rao, D. S. S.; Prasad, S. K.; Babu, V. V. S. *Chem.—Eur. J.* **2008**, *14*, 10462−10471.
(39) Strictly speaking, we measure the combined current flow resulting from the conductance of our samples and the dielectric displacement (D), which consists of a vacuum and a material contribution. The polarization (P) refers to the part of the dielectric displacement that originates from the response of the material to the electric field only. Since we estimate the value of the spontaneous polarization of the BTAs by subtracting a baseline that takes both conductive and capacitive effects into account, we choose to use the term polarization throughout this paper to avoid confusion.
(40) Scott, J. F. *J. Phys.: Condens. Matter* **2008**, *20*, 021001.
(41) Kishikawa, K.; Nakahara, S.; Nishikawa, Y.; Kohmoto, S.; Yamamoto, M. *J. Am. Chem. Soc.* **2005**, *127*, 17962−17962.
(42) Matraszek, J.; Mieczkowski, J.; Pociecha, D.; Gorecka, E.; Donnio, B.; Guillon, D. *Chem.—Eur. J.* **2007**, *13*, 3377−3385.
(43) Francescangeli, O.; Stanic, V.; Torgova, S. I.; Strigazzi, A.; Scaramuzza, N.; Ferrero, C.; Dolbnya, I. P.; Weiss, T. M.; Berardi, R.; Muccioli, L.; Orlandi, S.; Zannoni, C. *Adv. Funct. Mater.* **2009**, *19*, 2592−2600.
(44) Hahn, H.; Keith, C.; Lang, H.; Reddy, R. A.; Tschierske, C. *Adv. Mater.* **2006**, *18*, 2629−2633.
(45) Horiuchi, S.; Tokura, Y. *Nat. Mater.* **2008**, *7*, 357−366.
(46) Lovinger, A. J. *Science* **1983**, *220*, 1115−1121.
(47) Furukawa, T.; Date, M.; Ohuchi, M.; Chiba, A. *J. Appl. Phys.* **1984**, *56*, 1481−1486.
(48) Haase, W.; Kilian, D.; Athanassopoulou, M. A.; Knawby, D.; Swager, T. M.; Wrobel, S. *Liq. Cryst.* **2002**, *29*, 133−139.
(49) Rochefort, A.; Bayard, E.; Hadj-Messaoud, S. *Adv. Mater.* **2007**, *19*, 1992−1995.
(50) Merz, W. J. *Phys. Rev.* **1954**, *95*, 690−698.
(51) Naber, R. C. G.; Blom, P. W. M.; de Leeuw, D. M. *J. Phys. D: Appl. Phys.* **2006**, *39*, 1984−1986.
(52) Vizdrik, G.; Ducharme, S.; Fridkin, V. M.; Yudin, S. G. *Phys. Rev. B* **2003**, *68*, 094113.
(53) Ishibash., Y; Takagi, Y. *J. Phys. Soc. Jpn.* **1971**, *31*, 506−510.
(54) See Supporting Information for a sample plot of the limiting current against the applied field showing the ohmic conduction in both BTAs.
(55) Fatuzzo, E.; Merz, W. J. *Phys. Rev.* **1959**, *116*, 61−68.
(56) Merz, W. J. *J. Appl. Phys.* **1956**, *27*, 938−943.
(57) Ishibashi, Y. *Jpn. J. Appl. Phys., Part 1* **1992**, *31*, 2822−2824.
(58) Orihara, H.; Ishibashi, Y. *Jpn. J. Appl. Phys., Part 1* **1984**, *23*, 1274−1277.
(59) See Supporting Information for data and detailed discussion.
(60) Angell, C. A. *Science* **1995**, *267*, 1924−1935.
(61) Glusen, B.; Kettner, A.; Kopitzke, J.; Wendorff, J. H. *J. Non-Cryst. Solids* **1998**, *241*, 113−120.
(62) Russell, E. V.; Israeloff, N. E. *Nature* **2000**, *408*, 695−698.
(63) Wurfel, P.; Batra, I. P. *Phys. Rev. B* **1973**, *8*, 5126.
(64) Batra, I. P.; Wurfel, P.; Silverman, B. D. *Phys. Rev. B* **1973**, *8*, 3257.
(65) Batra, I. P.; Silverman, B. D. *Solid State Commun.* **1972**, *11*, 291.
(66) Berardi, R.; Orlandi, S.; Zannoni, C. *J. Chem. Soc., Faraday Trans.* **1997**, *93*, 1493−1496.
(67) Ayton, G.; Patey, G. N. *Phys. Rev. Lett.* **1996**, *76*, 239−242.
(68) Weis, J. J.; Levesque, D.; Zarragoicoechea, G. J. *Phys. Rev. Lett.* **1992**, *69*, 913−916.
(69) Kishikawa, K.; Nakahara, S.; Nishikawa, Y.; Natsukawa, M.; Kohmoto, S. *Mol. Cryst. Liq. Cryst.* **2009**, *498*, 11−18.
(70) Kremer, F.; Schönhals, A. *Broadband dielectric spectroscopy*; Springer: Berlin, Germany, 2003.
(71) Wubbenhorst, M.; van Turnhout, J. *J. Non-Cryst. Solids* **2002**, *305*, 40−49.
(72) Starkweather, H. W. *Macromolecules* **1981**, *14*, 1277−1281.
(73) See Supporting Information for a complete overview of all relaxation processes and additional discussion.
(74) Yildirim, Z.; Wubbenhorst, M.; Mendes, E.; Picken, S. J.; Paraschiv, I.; Marcelis, A. T. M.; Zuilhof, H.; Sudholter, E. J. R. *J. Non-Cryst. Solids* **2005**, *351*, 2622−2628.
(75) Kremer, F. *J. Non-Cryst. Solids* **2002**, *305*, 1−9.
(76) Elmahdy, M. M.; Dou, X.; Mondeshki, M.; Floudas, G.; Butt, H. J.; Spiess, H. W.; Mullen, K. *J. Am. Chem. Soc.* **2008**, *130*, 5311−5319.
(77) Elmahdy, M. M.; Floudas, G.; Mondeshki, M.; Spiess, H. W.; Dou, X.; Mullen, K. *Phys. Rev. Lett.* **2008**, *100*, 107801.
(78) Leisen, J.; Werth, M.; Boeffel, C.; Spiess, H. W. *J. Chem. Phys.* **1992**, *97*, 3749−3759.
(79) See Supporting Information for the NMR data and additional discussion.